

# Optimization of Absolute Variable Reluctance Resolver with Taguchi and FEM

LongFei XIAO  
*Machinery Institute*  
*University of Shanghai for Science and Technology*  
 Shanghai, China  
 long.fei.xiao@foxmail.com

Chao BI  
*Machinery Institute*  
*University of Shanghai for Science and Technology*  
 Shanghai, China  
 bichao@usst.edu.cn

**Abstract**—As angle sensors, Variable Reluctance (VR) resolvers can be divided into incremental and absolute types (IVR and AVR). Both IVR and AVR resolvers have been widely used in many drive systems. However, high performance AVR resolvers are difficult to design as the effects of rotor shape is very complicated. In this paper, Taguchi method combines with FEM Finite Element Method (FEM) is used to optimize the accuracy of AVR resolver by adjusting the rotor shape. The optimization time can thus be reduced significantly.

**Keywords**—*Absolute Variable Reluctance resolver, Taguchi, FEM, optimization, position error*

## I. INTRODUCTION

Driven by the requirement for high-performance motion control systems, absolute rotor-position signals have been concerned in many applications related with control system [1]-[3].

Among angle transducers, optical absolute encoders and AVR resolvers are the important solutions in realizing the precise absolute-position sensing.

Optical encoders are widely used in many applications. This kind of sensors utilize optical principle has extremely high accuracy. In addition, the processing of digital outputs is relatively easier than AVR resolver [4]. However, the adoption of optical absolute encoders is full of worries. There are several restrictions on optical encoders [5],[6]. The main serious defects existing in them are poor anti-interference, fragility, complicated structure and high manufacturing cost. In other words, quality-value ratio of optical absolute encoders is quite low especially for the applications like heavy machines.

By contrast, the performance of AVR resolvers is attractive and has been adopted in industry, especially in electric vehicles and robots. As the global electromagnetic (EM) effect is used, AVR resolvers have relatively small dimensions, low cost, great interference immunity and adaptability to the working environment. Nevertheless, the vast majority of papers about VR resolvers focus on IVR rather than AVR resolvers. The reason lies in the trouble of the rotor design. The main difference between them is that the rotor structure of AVR resolvers is eccentric, which is more complicated and harder to describe.

This paper gives some review on the design of rotor shapes in VR resolvers. Then, two geometric structure of the rotor in AVR resolvers are introduced. And the rotor shape is formulated based on Fourier series. Besides, the optimization algorithm combining both Taguchi method and FEM are introduced. Finally, an example for optimizing the AVR resolver with 10 slots is used to describe the algorithm.

## II. THE CONCEPT OF AVR RESOLVER

The basic principle of AVR resolver is similar to a transformer. As shown in Fig. 1, the exciting windings can be activated by high frequency current. When the shaft revolves, the appropriate rotor shape can vary the flux linkage of the output windings in sinusoidal. Then the oscillating voltage signals which is related to sine and cosine functions of the rotor position is induced in two output windings. Finally, the precise rotor-position information could be decoded using resolver to digital (R/D) converter [7]-[9]. And, it's remarkable that AVR resolver and R/D Converter are indispensable and important components of the complete resolver position sensing system

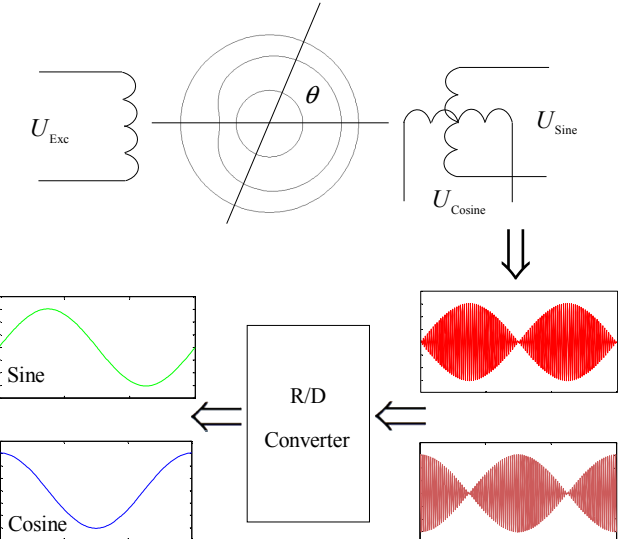


Fig. 1 The main principle of AVR resolver

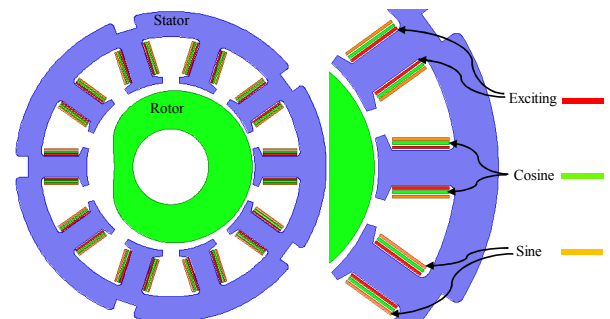


Fig. 2 The AVR resolver with 10 slots

Fig. 2 shows an example of AVR resolver of 10 slots. The stator structure is derived from a practical product. Besides, exciting and two output windings with alternate polarities are located in each stator tooth. In this combination of stator slot and rotor pole, the number of exciting winding

of each pole is uniform. While, the distribution of Sine and Cosine output windings is special and the calculation of them will be mentioned in another paper.

### III. REVIEW ON THE DEVELOPMENT OF ROTOR SHAPES IN VR RESOLVERS

#### A. Toothed rotor

The earliest VR resolver belongs to the IVR resolver. The structure of it is shown in Fig. 3, which bears similarity to the VR stepper motor [10].

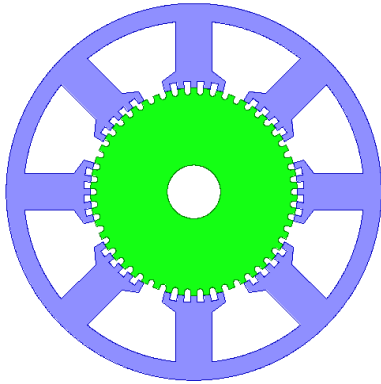


Fig. 3 The earliest VR resolver

In earlier designs, the most important component of conventional VR resolvers is the teeth. In order to guarantee high precision, the number of teeth should be large. What's more, careful consideration should also be given to the tooth geometry such as tooth-width/tooth-pitch ratios and slot-depth/tooth-pitch ratios. Manufacturing costs remain high and performance is difficult to ensure, so that toothed rotor is eventually eliminated.

#### B. Lobed rotor

For getting rid of the above constraints of the toothed rotor, the lobed rotor emerged. As shown in Fig. 4 and Fig. 5, one or more lobes arranges around the rotor.

Compared with the IVR rotor, there is only one lobe in the AVR rotor. In other words, the rotor structure of AVR resolvers is eccentric. Moreover, the geometries of the rotor in AVR resolvers can be classified into two categories. One is an eccentric circle, the other is heart-shaped, as shown in Fig. 5.

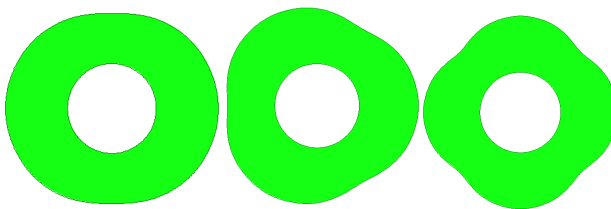


Fig. 4 The rotor shapes of IVR resolvers

The lobed rotor can make the variation of the airgap permeance close a sinusoidal variation, which is the critical impact constraint of the accuracy of output signals. However, the difficulty of rotor design is increased. As it is mentioned, the design and optimization of the toothed rotor are both centered on tooth parameters. By contrast, the lobed rotor lacks clear structural parameters, which make it hard to describe the shape curve by formulation.

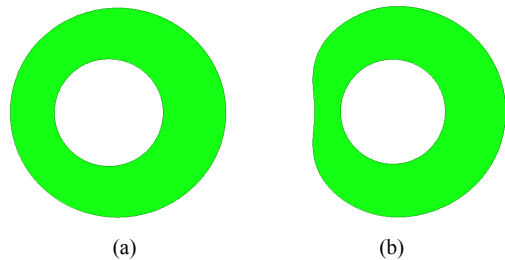


Fig. 5 Two types of rotor shapes in AVR resolvers. (a) eccentric circle (b) heart-shaped.

#### C. Reviews on the design of lobed rotor

In the past decades, the researches of AVR resolver went through several stages. In authors' opinion, the primitive AVR lobed rotor may be similar to the one as shown in Fig. 6. And the lobes of resolvers can be expressed by

$$\begin{cases} r = a + b \times \sin(p \times \theta / 2) \\ \theta \in [0, 2\pi / p] \end{cases}, \quad (1)$$

where,  $p$  is the number of rotor lobes,  $r$  and  $\theta$  represent the rotor radius and the rational angle respectively.

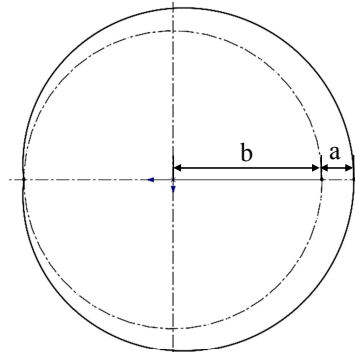


Fig. 6 Primitive AVR lobed rotor

Some designers who entirely depend on their rich practical experience combine (1) with other curve functions such as hyperbola and asymptote to obtain an passable curve of the lobed rotor. However, this is not practical in many applications.

A number of designers get the proper rotor shape based on the analysis of the airgap permeance [10]-[13]. However, such analysis is full of difficulties and time-consuming as EM structure becomes complexity. Neither magnetic circuit method nor FEM can simply complete the calculation of airgap permeance.

From our point of view, the design of the lobed rotor should be divided into two parts: initial scheme and optimization process. A minority of designers adopted this strategy. The initial scheme is a key issue which puts serious impact on the subsequent optimization. [14] proposed a length function with a fundamental wave factor and an auxiliary third-harmonic factor. But, there are still some shortcomings. The main problem is that the selection of initial parameters based on the analysis of voltage harmonics is relative time-consuming.

#### IV. LOBED ROTOR BASED ON FOURIER SERIES

In this section, the rotor radius of VR resolvers based on Fourier series is further investigated, which can be

expressed by

$$r(\theta) = h_0 + \sum_{i=1}^{\infty} h_i \cos(ip\theta) , \quad (2)$$

where  $h_i$  and  $h_0$  are the form factors of the rotor shape.

According to (2), this paper proposes the initial models of two types of rotor shapes in AVR resolvers, as shown in Fig. 7. The form factors which can be set roughly without calculation in initial models will be optimized by the Taguchi method. And the process of optimization is illustrated below.

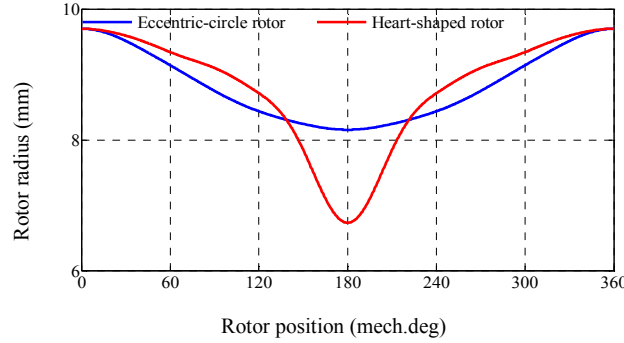


Fig. 7 Two types of lobed rotors in AVR resolvers

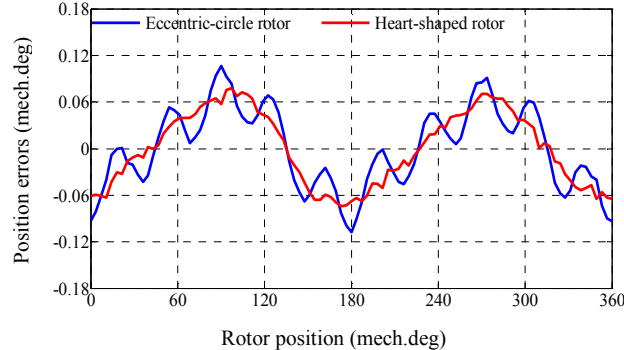


Fig. 8 The optimal results of types of lobed rotors (FE results)

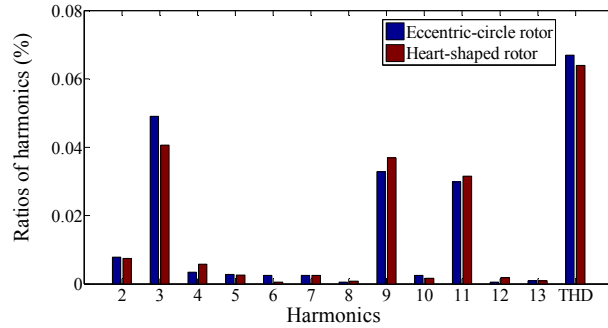


Fig. 9 Voltage harmonics for AVR resolvers with two types of lobed rotors

Fig. 8 shows the optimal results of the eccentric-circle rotor and heart-shaped rotor in FEM. Fig. 9 indicates the voltage harmonics of the output signals between two types of lobed rotors. According to the process of optimization and the FE results, the heart-shaped rotor seems to be easier to get high precision. However, this phenomenon also indicates the heart-shaped rotors' sensibility to the variation of shape factors. By contrast, the eccentric-circle rotor has better robustness. In other words, the heart-shaped rotor is appropriate in the presence of superb processing conditions.

And, the eccentric-circle rotor may be a proper choice under the condition of insufficient technology.



Fig. 10 Prototype of the AVR rotor optimized

As the limitation in the paper length, further research and testing results of the two types of will be illustrated in another paper.

## V. OPTIMIZATION OF AVR ROTOR SHAPES

### A. FEM Model

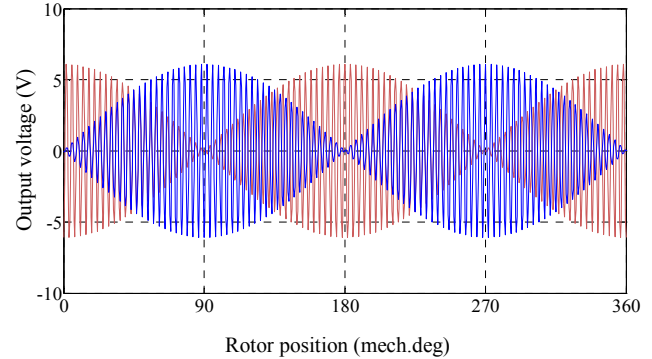


Fig. 11 The output signals in 2D transient model

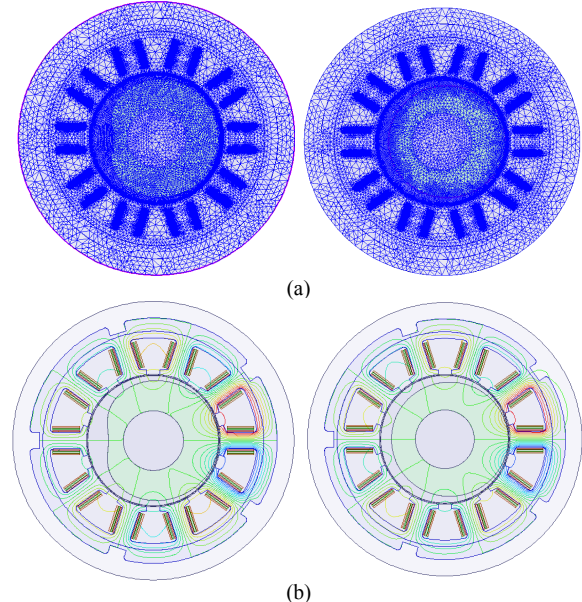


Fig. 12 FEM model. (a) Finite element meshing diagram. (b) Flux lines.

The output signals in 2D transient model is oscillating as shown in Fig. 11. It is inconvenient for designers to analysis the angle errors. In order to eliminate the decoding process and reduce the simulation time, the 2D eddy current model

of the AVR resolver is adopted, as shown in Fig. 12. The 2D eddy current model can directly achieve the Sine and Cosine voltage signals which are illustrated in Fig. 13. In this model, the exciting current can be expressed by

$$i_e = 0.032 \times N_{EXC} = 0.032 \times 27 = 0.864A , \quad (3)$$

where  $N_{EXC}$  represents the turns of exciting windings on each tooth.

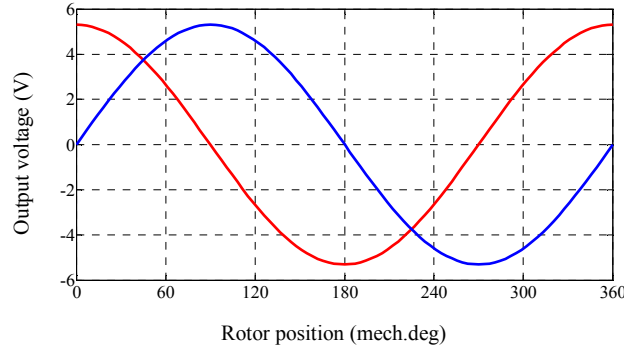


Fig. 13 The output signals in 2D eddy current model

### B. Taguchi Optimization Method

In recent years, industrial circles have utilized Taguchi method to achieve robust designs based on a small number of experiments.

Taguchi optimization method which uses the discrete results to explore the optimal point has proved to be more cost-effective alternative to conventional experiments [15]-[17]. The reason lies in Orthogonal Table and Signal to Noise ratio (S/N ratio). The former is valid for the reduction of FEA calculation number. The latter is the key to the analysis of factors' effect proportion and optimal selection.

Fig. 14 shows the basic process of Taguchi optimization method. At first, it is necessary to select an objective function about mechanical angle errors of the rotor. It can be expressed by

$$\text{Position error} = \max |error(i)| , \quad (4)$$

where,  $error(i)$  represents the electrical angle error between the calculated value and the ideal value.

Besides, this paper also adopts an auxiliary function about total harmonic distortion (THD), which is expressed by

$$\text{THD} = \sqrt{\sum_{n=2}^{\infty} V_n^2} / V_1 , \quad (5)$$

where,  $V_1$  is the fundamental wave of output voltage,  $V_n$  are other harmonics except the fundamental wave.

Gen'ichi who is the initiator of the Taguchi method proposed three formulations for calculating the S/N ratio and a number of orthogonal arrays. The orthogonal table which is selected in this paper is shown in TABLE I, and the formulation adopted in this paper is expressed by

$$SN_i = -10 \log \left[ \left( \sum_{i=1}^n y_i^2 / n \right) \right] , \quad (6)$$

where,  $y_i$  represents the result of the  $i^{th}$  combination of factor levels and  $n$  is the number of experiments based on the  $i^{th}$  combination.

Four shape factors with three levels of heart-shaped rotor are selected in the orthogonal table where  $A = h_2$ ,  $B = h_3$ ,  $C = h_4$ ,  $D = h_5$ .

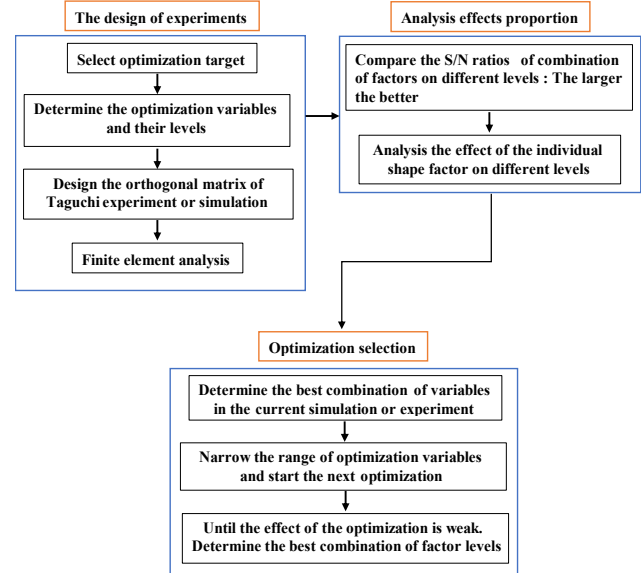


Fig. 14 The basic process of Taguchi optimization method

TABLE I  
THE SIMULATION RESULTS OF HEART-SHAPED ROTOR IN FIRST STAGE

No	Factor				THD (%)	Position error (elec. deg)	S/N
	A	B	C	D			
1	1	1	1	1	0.1303	0.1292	17.770
2	1	2	2	2	0.1380	0.1233	18.180
3	1	3	3	3	0.1196	0.1193	18.466
4	2	1	2	3	0.0664	0.0905	20.863
5	2	2	3	1	0.1451	0.1386	17.167
6	2	3	1	2	0.1364	0.1338	17.469
7	3	1	3	2	0.0816	0.0999	20.009
8	3	2	1	3	0.0803	0.0927	20.661
9	3	3	2	1	0.1266	0.1316	17.614

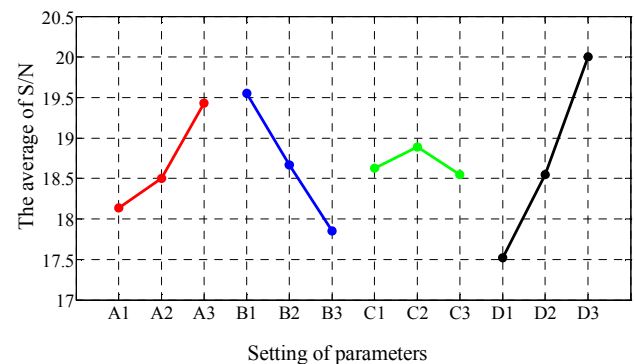


Fig. 15 The main effect diagram of S/N of shape factors in the first stage

The S/N ratios of combination of initial factors on different levels are reflected in TABLE I. In addition, the impact of the individual shape factor in first stage is shown in Fig. 15. D has the greatest influence, A, B take the second place and C is the weakest factor in first stage. According to the principle that the S/N ratio should be maximum, the best combination of factor levels in first stage is A3B1C2D3.

TABLE II  
THE SIMULATION RESULTS OF HEART-SHAPED ROTOR IN SECOND STAGE

No	Factor				THD (%)	Position error (elec. deg)	S/N
	A	B	C	D			
1	1	1	1	1	0.0692	0.1027	19.772
2	1	2	2	2	0.0644	0.0934	20.591
3	1	3	3	3	0.0571	0.0982	20.153
4	2	1	2	3	0.0543	0.0819	21.729
5	2	2	3	1	0.0674	0.0863	21.274
6	2	3	1	2	0.0637	0.0906	20.854
7	3	1	3	2	0.0626	0.0899	20.919
8	3	2	1	3	0.0586	0.0801	21.922
9	3	3	2	1	0.0633	0.1002	19.979

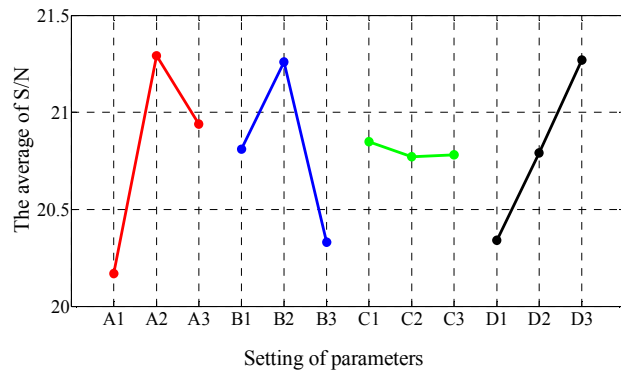


Fig. 16 The main effect diagram of S/N of shape factors in the second stage

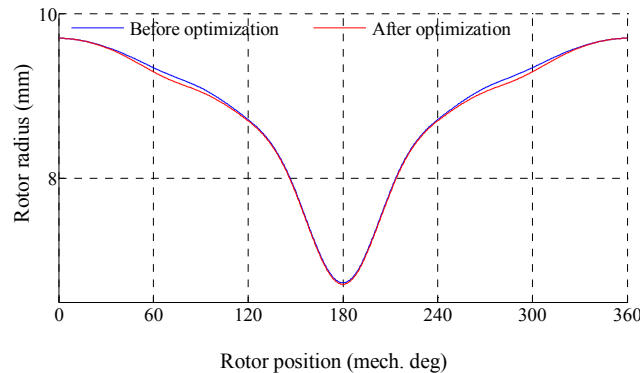


Fig. 17 The heat-shaped rotor before and after optimization

Narrowing the range of optimization variables and the combination of the final optimization (A2B2C1D3) is indicated in TABLE II and Fig. 16, and the optimal curve of the rotor is illustrated in Fig. 17.

Satisfactory results of Taguchi optimization Method are reflected in Fig. 18 where the THD of the AVR resolver with the heart-shaped rotor is decreased from 0.1072% to 0.0639% and the rotor-position errors are declined from  $0.1190^\circ$  to  $0.0757^\circ$ .

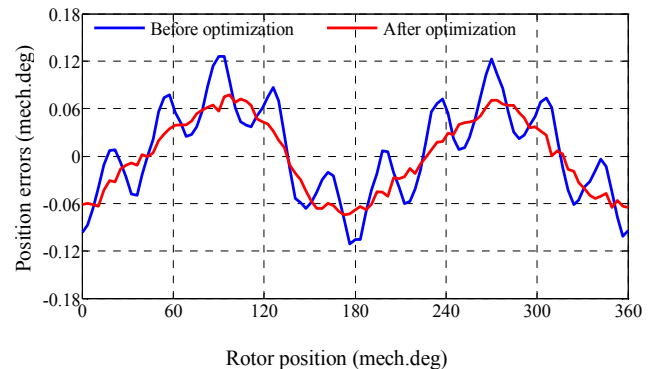


Fig. 18 Position errors of the AVR resolver with heart-shaped rotor (FE results)

## VI. CONCLUSION

The EM structure of AVR resolver is so complicated that the rotor shape is very hard to be described by conventional methods. This paper proposes the construction method of initial scheme of two types of lobed rotors in AVR resolvers. The curve can be described by Fourier series.

Taguchi optimization method with FEM are suitable for exploring the best point of the optimization with discrete objective function values. The angle precision can be directly improved by adjusting the factors of the lobed rotor. The FE results present in this paper confirmed the effectiveness in using this optimization approach. In addition, it can also be adopted in other VR resolvers and VR motors.

## REFERENCES

- [1] Ashok Nagarkatti, etc. "Harmonically graded air airgap reluctance-type rotating electric resolver," US Patent 4631510, 1986212223.
- [2] L. Harnefors and H.P. Nee, "A General Algorithm for Speed and position Estimation of AC Motors ", IEEE Trans. On Industrial Electronics, Feb. 2000, Vol.47(1):77-83
- [3] J.W. Ahn, "Torque control strategy for high performance SR drive," J. Electr. Eng. Technol., vol. 3, no. 4, pp. 538–545, 2008.
- [4] L. Sun, "Analysis and improvement on the structure of variable reluctance resolvers", IEEE Trans. Magn., vol. 44, no. 8, pp. 2002-2008, Aug. 2008.
- [5] L. Sun, J. Shang, J. Zou, "New absolute rotor-position sensors for inverter-driven motors", Proc. IEEE INTERMAG Conf., pp. 975-976, 2005.
- [6] LongFei Xiao, Zheng Li, Chao Bi, "Optimization of a Reluctance Resolver", 2018 Asia-Pacific Magnetic Recording Conference (APMRC)
- [7] A. Murray, B. Hare, A. Hirao, "Resolver position sensing system with integrated fault detection for automotive applications", Proc. IEEE Sensors, vol. 2, pp. 864-869, 2002-Jun
- [8] D. C. Hanselman, "Resolver signal requirements for high accuracy resolver-to-digital conversion", IEEE Transactions on Industrial Electronics, vol. 37, no. 6, pp. 556-561, 1990.
- [9] L. Z. Sun, Y. P. Lu, "Rotor-position sensing system based on one type of variable-reluctance resolver", Industrial Electronics Society 2006-32nd Annual Conference of IEEE, pp. 1162-1165, Nov. 200
- [10] D. C. Hanselman, R. E. Thibodeau, D. J. Smith, "Variable-reluctance resolver design guidelines", Proc. IECON'89, pp. 203-208, 1989.
- [11] S. Cui, H. Ge, "Stator structure design and analysis of variable reluctance resolver for hybrid-vehicle motor drive", Proc. 7th Int. Power Electron. Motion Control Conf., pp. 2587-2592, Jun. 2012
- [12] K. Kim, "Analysis on the characteristics of variable reluctance resolver considering uneven magnetic fields," IEEE Trans. Magn., vol. 49, no. 7, pp. 3858-3861, Jul. 2013.
- [13] X. Ge, Z. Q. Zhu, R. Ren, and J. T. Chen, "Analysis of windings in variable reluctance resolver," IEEE Trans. Magn., vol. 51, no. 5, May 2015, Art. no. 8104810.

- [14] X. Ge, etc, "A Novel Design of Rotor Contour for Variable Reluctance Resolver by Injecting Auxiliary Air-Gap Permeance Harmonics", *IEEE Trans. Energy Convers*, vol. 31, no. 1, pp. 345-353, 2016.
- [15] Ikuo Tanabe, "Development of a Tool for the Easy Determination of Control Factor Interaction in the Design of Experiments and the Taguchi Methods", 2017 International Conference on Control, Artificial Intelligence, Robotics & Optimization, pp. 301-306, 2017.
- [16] Tsili, M.A., Amoiralis, E.I., Kladas, A.G., et al.: 'Optimal design of multiwinding transformer using combined FEM, Taguchi and stochasticdeterministic approach', *IET Electr. Power Appl.*, 2012, 6, (7), pp. 437-454
- [17] I. Arizono, A. Kanagawa, H. Ohta, K. Watanabe, "Variable sampling plans for normal distribution indexed by Taguchi's loss function", *Naval Research Logistic*, vol. 44, no. 6, pp. 591-603, 1997.